POLITECNICO
MILANO 1863

SCUOLA DI INGEGNERIA INDUSTRIALE
E DELL'INFORMAZIONE

Executive Summary of the Thesis

Qualitative study of ballistic capture at Mars via Lagrangian descriptors

Laurea Magistrale in Space Engineering - Ingegneria Spaziale

Author: Alessio Quinci

Advisor: Prof. Francesco Topputo

Co-advisor: Gianmario Merisio

Academic year: 2020-2021

1. Introduction

Ballistic capture orbits have been receiving increasing attention throughout the past few decades. The reason is that they have the capability to reduce fuel requirements and provide more flexibility in terms of insertion opportunities and launch windows as compared to a typical patched-conics Keplerian approach [4].
An effective method to design ballistic capture orbits is based on stable sets manipulation, which revolves around simple algorithmic stability definitions [3, 4]. The method relies on sampling the phase space around the target planet and integrating a large number of orbits while checking if stability conditions are satisfied. The basic drawback is the brute-force nature of this approach, which is in general computationally intensive.
A new approach to ballistic capture can be found within the field of fluid dynamics. Lagrangian coherent structures (LCSs) are time-evolving structures in the phase space of a generic dynamical system which separate regions with qualitatively different dynamic behaviour [2]. Lagrangian descriptors (LDs) were recently introduced as a powerful visual tool capable to unveil LCSs [5]. The simple idea behind LDs is to seed a given phase space region with initial conditions (ICs) and integrate a bounded, positive property of the generated trajectories for a finite time. The boundaries between phase space regions comprising trajectories of different dynamical nature should denote singular structures with discontinuous spatial derivative in the LD field.
Aim of this study is to analyze to what extent LDs provide a characterization of the dynamics in Mars proximity with regard to ballistic capture. Motivations rely on the fact that LDs have the potential to be an efficient and easy to be implemented visual tool that could give a rich understanding of dynamics around the target planet. Research objective is to exhibit the correlation between the geometrical template extracted from LD fields in the phase space and the boundaries of subsets of ICs with peculiar behaviour obtained with stable sets manipulation. In this study, the boundaries are denoted as weak stability boundaries (WSBs), according to the nomenclature used in literature [3].

2. Dynamical model

The presented study is performed under the assumptions of the elliptic restricted three-body

problem (ER3BP) [3]. The model describes the dynamics of a massless particle which moves under the gravitational attraction of two primary bodies (P_1 with mass m_1, and P_2 with mass m_2) without influencing their motion. The two primaries motion is influenced only by their mutual attraction, being the solution of the two-body problem. The ER3BP is a natural generalization of the circular problem in which primaries orbit on ellipses with eccentricity e_p around their barycenter. ER3BP equations of motion can be expressed in a non-uniformly rotating, barycentric, non-dimensional coordinate frame where P_1 and P_2 have fixed positions $(-\mu, 0)$ and $(1-\mu, 0)$, respectively. $\mu = m_2/(m_1 + m_2)$ is the mass parameter of the system. This reference frame is also called synodic frame. Assuming planar motion of the third particle, ER3BP dynamics expressed in the non-dimensional synodic frame reads [3]

$$\begin{cases} x'' - 2y' = \omega_x, & \text{(1a)} \\ y'' + 2x' = \omega_y. & \text{(1b)} \end{cases}$$

Subscripts denote the partial derivatives with respect to x and y of

$$\omega(x, y, f) = \frac{\Omega(x, y)}{1 + e_p \cos f}, \tag{2}$$

where Ω is the potential function of the CR3BP. Primes in Eq. (1) represent differentiation with respect to the true anomaly f, which is the independent variable of the system and covers the role of time [3].

3. Methodology

LD approach is now applied to the Sun–Mars ER3BP to show the correlation between dynamics separatrices extracted from LD fields and the WSBs of classification sets.

3.1. Classification sets definition

The general procedure to categorize a certain phase space region of ICs in the domain of interest derives from the one described in [4]. An alternative formulation of sets is proposed. While propagating ICs in the non-dimensional synodic reference frame in the integration interval $[f_0, f_f]$, a classification algorithm computes the non-dimensional distance r and Kepler energy H of the particle with respect to Mars. Categorization is based on the fulfillment of some conditions that take distance and energy as input and verify if the particle escapes from the planet or impacts on its surface. With this procedure every initial state is collocated in one of three complementary subsets ($\mathcal{X}$, $\mathcal{K}$ or $\mathcal{W}$) depending on its dynamics. Classification sets are defined in the following list:

Escape set $\mathcal{X}(f_f)$ contains ICs whose orbits escape for $f \leq f_f$. The particle escapes if it possesses positive Kepler energy and, at the same time, is located outside planet sphere of influence. The two conditions that must be satisfied at the same time are

$$\begin{cases} H(f) > 0, & \text{(3a)} \\ r(f) > R_s, & \text{(3b)} \end{cases}$$

where R_s is the non-dimensional sphere of influence radius of Mars.

Crash set $\mathcal{K}(f_f)$ contains ICs whose orbits crash for $f \leq f_f$. The particle impacts if its distance from Mars surface is negative, or equivalently

$$r(f) < R_{eq}. \tag{4}$$

R_{eq} represents the non-dimensional mean equatorial radius of the planet.

Weakly stable set $\mathcal{W}(f_f)$ contains ICs whose orbits do not escape or crash for $f \leq f_f$.

In analogy with the capture set definition given in [4], an alternative formulation of is derived. A capture set $\mathcal{C}(f_B, f_F)$ is extracted from the intersection between an escape set $\mathcal{X}$ obtained propagating dynamics backwards and a weakly stable set $\mathcal{W}$ obtained integrating forwards.

$$\mathcal{C}(f_B, f_F) = \mathcal{X}(f_B) \cap \mathcal{W}(f_F). \tag{5}$$

An IC belonging to $\mathcal{C}(f_B, f_F)$ generates an orbit that escapes from the target planet before reaching f_B if integrated backwards, while remains bounded into the region of influence of Mars without crashing at least until f_F if integrated forwards. ICs inside a capture set can be exploited to design ballistic capture orbits.

3.2. LDs computation

LD definition adopted in the study case reads

$$M(\mathbf{x}_0, f_0, f_F, f_B) = \int_{f_0 - f_B}^{f_0 + f_F} |\mathcal{F}(\mathbf{x}(f))|^\gamma \mathrm{d}f. \tag{6}$$

$\mathbf{x} = [x, y, x', y']$ denotes the state vector of the problem and it is retrieved rearranging Eq. (1) as a four-dimensional ordinary differential equations system expressed as $\mathbf{x}' = \mathbf{f}(\mathbf{x}, f)$. Each IC is initially set at the periapsis of an osculating prograde ellipse around Mars, with a given eccentricity $e = 0.9$ at $f_0 = 0$. From this assumption the full initial state $\mathbf{x}_0$ of the particle can be retrieved [3].
Integrand $|\mathcal{F}(\mathbf{x}(f))|^\gamma$ denotes a bounded, positive property of the state vector, with γ the exponent that defines its norm. Different integrands have been implemented and tested. A $\mathcal{F} = [x', y']$ with $\gamma = 1/2$ gives a clear visual separation of phase space regions in the LD field. The associated descriptor is labeled as M_3.
LD field is generated evaluating the integral per each $\mathbf{x}_0$ in a computational grid G of ICs in the domain of interest, so every grid point in the phase space is linked to a positive scalar value. $M(G, f_0, f_F, f_B)$ represents the LD field computed for all the grid points. A contour plot in the position subspace (x, y) is then performed to underline some boundaries, denoted by "abrupt changes" of the field. An abrupt change means that the derivative of M field transverse to the boundaries is discontinuous on them. These singular features coincide with phase space structures that separate orbits with different dynamics. Notice that LD definition $M(\mathbf{x}_0, f_0, f_F, f_B)$ can be splitted in two contributions. Forward contribution $M(\mathbf{x}_0, f_0, f_F, 0)$ isolates dynamics separatrices generated in forward time which are linked to repelling LCSs of the dynamical system. Similarly, $M(\mathbf{x}_0, f_0, 0, f_B)$ highlights the attracting LCSs of the system, isolating separatrices in backward time.

3.3. Separatrices extraction

Singular structures revealed by LD fields are extracted with an edge detection algorithm. Edge detection is an image processing technique usually exploited for finding boundaries of objects within images. An edge is defined as the locus of points in which there is a rapid change in intensity of the image. There are several edge detection algorithms which differ for their criterion with whom they detect discontinuities. Some of them are Sobel, Prewitt, Roberts, Canny and zero-cross methods [1]. Different methods have been tested for this study case. Roberts proved to be the most effective one by revealing the edges more clearly than the other methods. The algorithm takes as input the two-dimensional contour plot of the descriptor field in the (x, y) subspace of the domain. Then it finds edges at those points where the gradient magnitude of the image is higher than a threshold value using the Robert approximation to the derivative [1]. As previously introduced, an additional input of edge detection algorithms is the sensitivity threshold σ. For gradient magnitudes higher than the threshold, algorithm ignores those edges. Edge detection gives as output a binary image of the same size of LD scalar field, with 1s where the algorithm finds edges and 0s elsewhere. Per each computed descriptor field the value of threshold is tuned in order to show the highest number of structures associated to abrupt changes in the field. However, too low values of the threshold itself could generate false positives in the output binary image when compared to the LD contour plot. Chosen thresholds associated to computed LD fields are reported in Tab. 1.

Table 1: Computed descriptor fields and associated thresholds.

LD field	σ
$M_3(G, 0, \pi/2, 0)$	$4 \cdot 10^{-3}$
$M_3(G, 0, \pi, 0)$	$6 \cdot 10^{-3}$
$M_3(G, 0, 3\pi/2, 0)$	$9 \cdot 10^{-3}$
$M_3(G, 0, 2\pi, 0)$	$20 \cdot 10^{-3}$
$M_3(G, 0, 5\pi/2, 0)$	$25 \cdot 10^{-3}$
$M_3(G, 0, 3\pi, 0)$	$30 \cdot 10^{-3}$
$M_3(G, 0, 0, -\pi/2)$	$4 \cdot 10^{-3}$
$M_3(G, 0, 0, -\pi)$	$6 \cdot 10^{-3}$

3.4. Validation of separatrices

Ideally, extracted dynamics separatrices from LD fields should match exactly with the WSBs of classification sets $\mathcal{X}$, $\mathcal{K}$ and $\mathcal{W}$ for a given integration interval. Flowchart in Fig. 1 summarizes the workflow designed to validate extracted patterns. The first step is to build a computational grid of ICs around Mars. Two basic elements characterize it: boundaries of the domain of interest and number of grid points. The grid is built in the synodic frame centered at the target at f_0, which in this study is also referred as inertial frame for simplicity. The selected

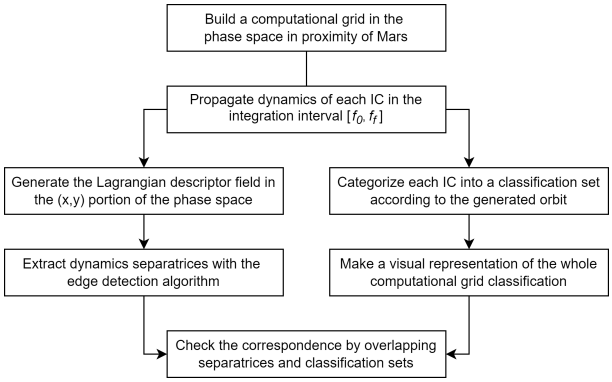

Figure 1: Validation workflow.

portion of (x, y) domain allow to appreciate the differences between classification sets computed at different f_f. Selected domain boundaries are $[-6\cdot10^{-4}, 6\cdot10^{-4}]\times[-6\cdot10^{-4}, 6\cdot10^{-4}]$. Number of grid points is selected as compromise between computational effort and visual quality of LD fields and classification sets. A value of $25 \cdot 10^4$ grid points is chosen. Each IC is then integrated in a given anomalies interval with a $7^{\text{th}}/8^{\text{th}}$ order Runge-Kutta scheme. Integration tolerance is set to 10^{-9}. Sun–Mars parameters are reported in Tab. 2.

Table 2: Sun–Mars parameters, taken from [3, 4].

Parameter	Value	Unit
μ	$3.2262008 \cdot 10^{-7}$	[−]
a_p	1.523688	[AU]
e_p	0.093418	[−]
R_{eq}	3397	[km]
R_s	$170 \cdot R_{eq}$	[km]

a_p and e_p are the semi-major axis and eccentricity of Sun–Mars system, respectively. Initial states are propagated in the $[f_0,\ f_f]$ interval. LD scalar values are computed and, at the same time, the classification algorithm categorize each IC into the subset $\mathcal{W}(f_f)$, $\mathcal{X}(f_f)$, or $\mathcal{K}(f_f)$. Separatrices are extracted from the contour plot of the descriptor field with the edge detection algorithm. Patterns are then overlapped to the computational grid classification, in which each subset is marked with a different colour. This allows to perform a visual check of the matching between WSBs and separatrices extracted from LD fields.

4. Results

An example of LD field computed for a given integration interval is shown in Fig. 2. Abrupt changes in the scalar values of the field correspond to dynamics separatrices. They are extractred with the edge detection algorithm and superimposed on the computational grid classification, as presented in Fig. 3.

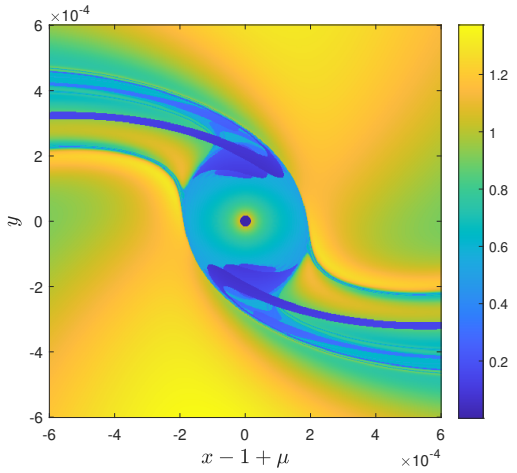

Figure 2: $M_3(G, 0, 2\pi, 0)$ field.

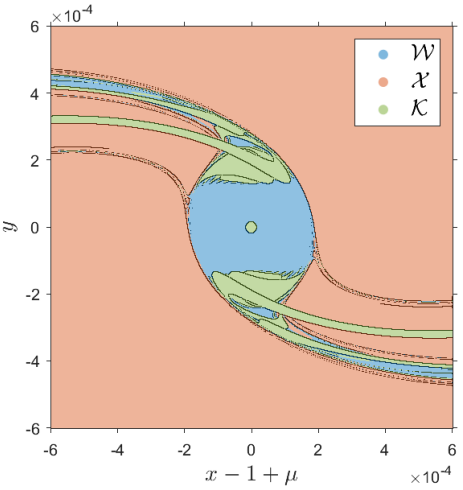

Figure 3: $M_3(G, 0, 2\pi, 0)$ field separatrices overlapped to classification sets computed at $f_f = 2\pi$.

A good match of separatrices with the boundaries of classified regions can be noticed. Two key points deserve mention. LD reveals patterns if ICs are integrated long enough for dynamic divergences between the orbits to be appreciated. It may happen that the classification algorithm divides a particular region of the phase space

into two different subsets, but the orbits are not so divergent to generate singular structures in the LD field. In this case we expect an high gradient in the field in correspondence of the WSB, but not sufficiently high to be detected by the edge detection algorithm. Another point is that LD may detect divergence in dynamic behaviour even in areas that are classified in the same way. For instance, two grid points can both generate crash orbits, but trajectories could be very different from each other. This usually happens at higher values of the integration limit. As rule of thumb, the higher the value of f_F, the more structures are revealed. An high value of f_F gives to trajectories enough time to manifest their qualitative behaviour.
Combining LD structures obtained propagating dynamics forwards with the ones obtained propagating backwards, it is possible to reveal patterns that rule particles transport in both time directions. The correlation of a capture set $\mathcal{C}(f_B, f_F)$ with extracted patterns from $M_3(G, 0, f_F, f_B)$ field can be recognized in Fig. 4. Some regions in the phase space which are enclosed by LD separatrices correspond, with reasonable approximation, to the capture set. ICs belonging to this set generate orbits that approach Mars from outside and remain temporary captured at least until f_F.

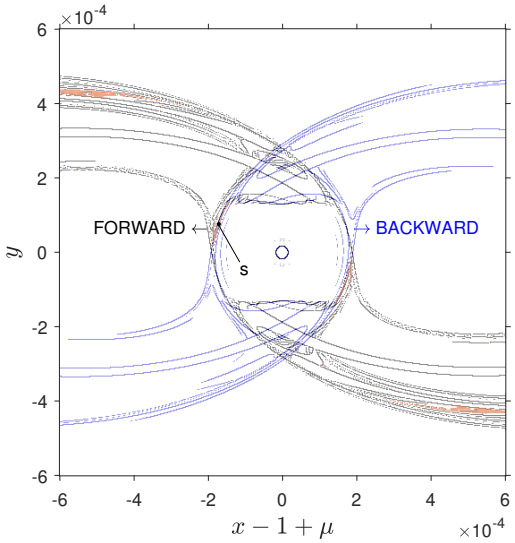

Figure 4: Extracted separatrices from $M_3(G, 0, 3\pi, -\pi)$ field overlapped to capture set $\mathcal{C}(-\pi, 3\pi)$. Gray lines are associated with the forward branch of the integral and blue lines with the backward one.

Fig. 5 shows the orbit generated from the IC "s" sampled from Fig. 4. As expected, particle approaches the planet from outside its sphere of influence (SOI) and remains bounded in the proximity of Mars at least for three semi-revolutions of the planet around the Sun.

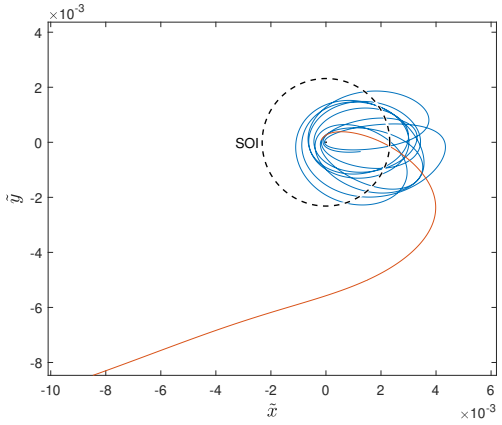

Figure 5: Orbit generated from IC "s" in the Mars-centered inertial frame (red path: backward propagation; blue path: forward propagation).

5. Conclusions

As shown in the results, structures in the phase space detected from LD fields are able to distinguish regions characterized by different dynamical behaviour. In particular, the patterns extracted with the edge detection algorithm delimit with good approximation the ICs that generate differently classified orbits. Extracted dynamics separatrices adequately match with the WSBs. Similarly, the LD approach detects areas corresponding to capture regions.
The main drawback of the LD approach is that it does not give information about which, among the different regions bounded by the structures, are actually capture or stable sets. This is a limitation in the application of the presented methodology to the design of ballistic capture orbits. The procedure of computing the LD fields, together with extraction and validation of the dynamics separatrices have had a positive response. Thus, based on the obtained results, a viable strategy to design ballistic capture orbits is proposed. A possible solution could be to categorize the various regions delimited by the extracted separatrices by sampling a few ICs and classifying their orbits. In this way, each region

in the phase space can be classified on the basis of its qualitative behaviour (weakly stable, escape, capture, or impact). The assumption under this procedure is that each IC of a phase space region bounded by separatrices belongs to the same classification set.
In conclusion, LD proved to be an intuitive, easy to implement and computationally efficient visual tool. Without any a priory knowledge, LD patterns yield a strong match with the WSB of classification sets. The LD technique supports the design of ballistic capture trajectories, enriching the dynamics knowledge in proximity of the target planet.
An important advantage of the LD methodology is that it can be applied to arbitrary complex dynamical systems without restrictions. Thus, the presented approach could be generalized for the application in real solar systems models such as the n-body problem including different orbital perturbations.

References

[1] S. Ansari, S. Prabhu, N. Kini, G. Hegde, and Y. Haider. A survey on conventional edge detection techniques. *International Journal of Scientific Research in Computer Science Applications and Management Studies*, 3, 2014.

[2] G. Haller. Lagrangian coherent structures. *Annual Review of Fluid Mechanics*, 47(1):137–162, 2015.

[3] N. Hyeraci and F. Topputo. Method to design ballistic capture in the elliptic restricted three-body problem. *Journal of Guidance, Control, and Dynamics*, 33:1814–1823, 2010.

[4] Z.-F. Luo, F. Topputo, F. Bernelli-Zazzera, and G.-J. Tang. Constructing ballistic capture orbits in the real solar system model. *Celestial Mechanics and Dynamical Astronomy*, 120:433–450, 2014.

[5] A. M. Mancho, S. Wiggins, J. Curbelo, and C. Mendoza. Lagrangian descriptors: A method for revealing phase space structures of general time dependent dynamical systems. *Communications in Nonlinear Science and Numerical Simulation*, 18(12):3530–3557, 2013.